Published in final edited form as:
J Neurochem. 2009 August ; 110(3): 990–1004. doi:10.1111/j.1471-4159.2009.06194.x.

Real-time Visualization of Cytoplasmic Calpain Activation and Calcium Deregulation in Acute Glutamate Excitotoxicity

Akos A. Gerencser[1,*], **Karla A. Mark**[1,*], **Alan E. Hubbard**[1,2], **Ajit S Divakaruni**[1], **Zara Mehrabian**[3,4], **David G. Nicholls**[1], and **Brian M. Polster**[1,3,4,5]

[1]Buck Institute for Age Research, Novato, CA 94945, USA

[2]School of Public Health, University of California, Berkeley, CA 94720, USA

[3]Department of Anesthesiology, University of Maryland School of Medicine, Baltimore, MD 21201, USA

[4]Trauma and Anesthesiology Research Center, University of Maryland School of Medicine, Baltimore, MD 21201, USA

[5]Program in Neuroscience, University of Maryland School of Medicine, Baltimore, MD 21201, USA

Abstract

Although calpain (EC 3.4.22) protease activation was suggested to contribute to excitotoxic delayed calcium deregulation (DCD) via proteolysis of Na^+/Ca^{2+} exchanger 3 (NCX3), cytoplasmic calpain activation in relation to DCD has never been visualized in real time. We employed a calpain fluorescence resonance energy transfer (FRET) substrate to simultaneously image calpain activation and calcium deregulation in live cortical neurons. A calpain inhibitor-sensitive decline in FRET was observed at 39 ± 5 min after DCD occurred in neurons exposed to continuous glutamate (100 μM). Inhibition of calpain by calpeptin did not delay the onset of DCD, recovery from DCD-like reversible calcium elevations (RCE), or cell death despite inhibiting α-spectrin processing by >90%. Na^+/Ca^{2+} exchangers reversed during glutamate exposure, the NCX antagonist KB-R7943 prolonged the time to DCD, and significant NCX3 cleavage following 90 min of glutamate exposure was not observed. Our findings suggest that robust calpain activation associated with acute glutamate toxicity occurs only after a sustained loss in calcium homeostasis. Processing of NCX3 or other calpain substrates is unlikely to be the primary cause of acute excitotoxicity in cortical neurons. However, a role for calpain as a contributing factor or in response to milder glutamate insults is not excluded.

Keywords

excitotoxicity; apoptosis; necrosis; NCX; NMDA; calpeptin

INTRODUCTION

Modes of cell death in acute and chronic neurodegenerative disorders are widely varied and brain-region selective pathology is frequently observed (Bredesen *et al.* 2006;Lin and Beal

Address correspondence to: Brian M. Polster Department of Anesthesiology University of Maryland School of Medicine 685 W. Baltimore St., MSTF 5-34 Baltimore, MD 21201, USA phone: (410) 706-3418 fax: (410) 706-2550 e-mail: bpolster@anes.umm.edu. Akos A. Gerencser Buck Institute for Age Research 8001 Redwood Blvd. Novato, CA 94945 phone: (415) 209-2273 fax: (415) 209-2232 e-mail: agerencser@buckinstitute.org.
*these authors contributed equally to this work

2006). Despite this variability there is a pervasive view that antagonizing Ca^{2+}-dependent calpain proteases is universally protective. Two ubiquitous isoforms, μ-calpain (EC 3.4.22.52) and m-calpain (EC 3.4.22.53), are implicated in neurodegeneration (Bevers and Neumar 2008). *In vitro*, these isoforms are activated by micromolar and millimolar concentrations of calcium, respectively. Although intracellular calcium in healthy neurons is generally ~100 nM and does not reach millimolar levels until complete loss of calcium homeostasis occurs (Randall and Thayer 1992;Nicholls 2004), calpain activation prior to calcium deregulation has been explained by close proximity to NMDA receptors (Hewitt *et al.* 1998;Adamec *et al.* 1998;Vanderklish *et al.* 2000), sodium-calcium exchangers (Araujo *et al.* 2007), or other routes of local calcium elevation (Friedrich 2004).

Calpain activation near glutamate receptors was reported within five minutes of NMDA receptor activation (Vanderklish *et al.* 2000;Lankiewicz *et al.* 2000). NMDA, α-amino-3-hydroxy-5-methylisoxazole-4-propionate (AMPA), and mGluR1 receptor subunits are initial targets of calpain processing (Guttmann *et al.* 2002;Simpkins *et al.* 2003;Wu *et al.* 2005;Xu *et al.* 2007;Yuen *et al.* 2007a;Yuen *et al.* 2007b). By ameliorating the extent of intracellular Ca^{2+} and Na^{+} elevation during short bursts of glutamate receptor overactivation, these initial proteolysis events may protect the neuron from "accidental excitotoxicity." In contrast, sustained glutamate receptor activation leads to the calpain-dependent processing of numerous substrates, many with deleterious consequences for cell survival. Substrates include the cytoskeletal proteins α-spectrin and microtubule-associated protein 2 (MAP2) (Siman and Noszek 1988;Springer *et al.* 1997), plasma membrane calcium ATPases (PMCAs) (Pottorf *et al.* 2006), calcineurin phosphotase (Wu *et al.* 2004), the cyclin-dependent kinase 5 activator p35 (Lee *et al.* 2000), and apoptosis-inducing factor (AIF) (Polster *et al.* 2005;Cao *et al.* 2007).

The point-of-no-return for a neuron succumbing to excitotoxic injury is generally considered the time at which intracellular calcium homeostasis is irreversibly lost, i.e. delayed calcium deregulation (DCD) (Nicholls 2004). Events that contribute to the onset of DCD are predicted to influence cell survival with an opportunity for therapeutic intervention. However, events that occur after DCD are predicted to influence the timing of cell death without altering its inevitability. Calpain processing of sodium-calcium exchanger (NCX) isoform 3 and loss of calcium extrusion capacity was directly implicated in the delayed calcium rise observed in glutamate-treated cerebellar granule neurons (Bano *et al.* 2005). However, the relative expression of cleavage-resistant NCX1 to NCX3 is higher in forebrain neurons as compared to cerebellar granule neurons (Kiedrowski *et al.* 2004) although granule neurons are more resistant to DCD (Brorson *et al.* 1995;Castilho *et al.* 1998;Stout *et al.* 1998;Vergun *et al.* 1999;Bano *et al.* 2005;Bolshakov *et al.* 2008). This raises the possibility that alternate mechanisms precipitate DCD in forebrain neurons before calpain-mediated loss of functional NCX3 limits calcium homeostasis.

In this study we tested the hypotheses that: 1) DCD can occur without calpain activation in primary cortical neurons exposed to an excitotoxic concentration of glutamate, and 2) calpain activation converts DCD from a reversible to an irreversible event. This was accomplished by conducting simultaneous live cell imaging of calpain activation and intracellular calcium deregulation, investigating the function and processing of NCX, and testing the efficacy of calpain inhibitors against DCD, DCD-like reversible calcium elevations (RCE), and cell death. Our results define major cytoplasmic calpain activation in forebrain neurons as a distinct event occurring downstream of DCD that is not required for acute glutamate toxicity.

MATERIALS AND METHODS

Materials

Tetramethylrhodamine methyl ester ($TMRM^+$), Fura-4F-AM, Fura-6F-AM, Fluo-4FFAM, SBFI-AM, lipofectamine 2000, Neurobasal medium, B27 supplement, and GlutaMAX were from Invitrogen (Carlsbad, CA). Ionomycin, calpeptin, and PD150606 were purchased from EMD Biosciences (San Diego, CA). Primary rabbit polyclonal antibody to NCX3 was a kind gift of Dr. Ken Philipson (UCLA, Los Angelos, CA). Mouse monoclonal antibody to β-actin (clone AC-74) was from Sigma (St. Louis, MO). Mouse monoclonal antibody to α-spectrin (MAB1622) was from Chemicon (Temecula, CA). The pYSCS plasmid was generously provided by Dr. Peter Vanderklish (The Scripps Research Institute, San Diego, CA). All other reagents were purchased from Sigma unless otherwise indicated.

Preparation of primary neurons

Primary cortical neurons were prepared from 1-2 pairs of E18 rat cortices (BrainBits™, LLC, Springfield, IL) by papain dissociation followed by gentle trituration and used at 11-14 days in vitro (DIV). Briefly, cortices were washed in 2 ml of Hibernate™ medium (BrainBits™) and then digested with 2 mg/ml papain (Worthington) in Hibernate™ for 30 min at 37° C. Tissue was dispersed manually by 5-10 strokes with a 1 ml pipette and cells were plated onto poly-D-lysine-coated Lab-Tek 8-well chambered coverglasses (Nunc) at a density of 1×10^5cells/well. Cells were initially plated in Neurobasal medium containing B27 supplement (2%), L-glutamine (0.5 mM), fetal bovine serum (1%), penicillin (100 IU/ml) and streptomycin (100 μg/ml). For the majority of experiments, neurons were maintained at 37°C in an oxygen-regulated incubator with a humidified atmosphere of 92% N_2/5% CO_2/3% O_2. Every 3-4 days after the initial plating half of the medium was replaced with fresh medium lacking serum and containing GlutaMAX (0.5 mM) in place of L-glutamine. When stated, results with neurons cultured at physiologically relevant 3% O_2 (Grote *et al.* 1996) were confirmed using neurons cultured in a conventional 95% air/5% CO_2 environment. All experiments were conducted in room air.

Wide-field functional imaging

For simultaneous assay of DCD and calpain activation, cortical cultures were transfected with the pYSCS FRET sensor (Vanderklish *et al.* 2000) on day 9 using Lipofectamine 2000 (Invitrogen) in Neurobasal medium at a 3:2 ratio of Lipofectamine (αl) to DNA (αg); 0.2αg of DNA was transfected per well in 8-well Lab-Tek chambers. Experiments were carried out at 3 days post-transfection (at 12 DIV). The pYSCS transfected cultures were incubated with Fura-6F-AM (3 αM; Molecular Probes / Invitrogen) for 25 min at 37°C in imaging medium containing (in mM): 120 NaCl, 3.5 KCl, 1.3 $CaCl_2$, 0.4 KH_2PO_4, 20 *N*-Tris-(hydroxymethyl)-methyl-2-amino-ethanesulphonic acid (TES), 5 $NaHCO_3$, 1.2 Na_2SO_4, 15 D-glucose, the pH was set to 7.4 by NaOH (considering a pKa of 7.5 for TES, by 8.9 mM NaOH, yielding $[Na^+]_e$=136mM). For dye loading or in experiments with superfusion the imaging medium was supplemented with $MgCl_2$ (1 mM).

To image initial glutamate-triggered ionic changes, untransfected cortical cultures were incubated with Fura-4F-AM (1 μM; Molecular Probes / Invitrogen) for 20 min or with SBFI-AM (6 μM; in the presence of 0.02% Pluronic F127) for 40 min at 37°C in Mg^{2+}-supplemented imaging medium and subsequently rinsed. To monitor plasma membrane potential ($\Delta\Psi_P$), the plasma membrane potential indicator (PMPI; Molecular Devices #R8042 FLIPR Membrane Potential Assay Kit) was used at 1:200 dilution of the *Loading Buffer* (specified by the manufacturer).

Imaging was performed on an Olympus IX-81 inverted microscope equipped with a UAPO 20x air 0.75NA lens, a Lambda LS Xe-arc light source (175W), Lambda 10-2 excitation and emission filter wheels (Sutter Instruments, Novato, CA), a ProScan linear-encoded *xy*-stage (Prior, Rockland, MA) and a Coolsnap HQ cooled digital CCD camera (Photometrics, Tucson, AZ). The filter sets given as excitation-dichroic mirror-emission (in nm) were: for YFP or PMPI 500/24 (band pass) - 520LP (long pass) - 542/27 (Semrock, Rochester, NY), for CFP 438/24 - 458LP - 483/32 (Semrock), for FRET 438/24 - 458LP - 542/27 (Semrock) and for Fura dyes and SBFI 340 or 380 (Chroma, Rockingham, VT) - 458LP - 420LP. The whole microscope was maintained at 37°C in air using an environmental enclosure.

Measurement of the kinetics of calpain activation and DCD

Image acquisition was controlled by the Multi-Dimensional Acquisition application in Metamorph 6.3 (Molecular Devices). Images were recorded by using an ND1.0 (neutral density) attenuator, 100-200 ms exposure times and 3×3 binning in 2 minute intervals in 12 view fields at the following 5 wavelengths (defined above): YFP, CFP, FRET, Fura 340 and 380 nm. In each acquisition cycle the sample was auto-focused on green fluorescent beads placed in an empty well of the 8-well chamber. Fluorescence intensities were determined over the soma of pYSCS-expressing neurons after background subtraction. The background was defined by the peak of the intensity histogram of each frame. All of the following calculations were done by the region of interest (ROI) average intensities, except for images and videos shown, where calculations were performed pixel-by-pixel.

The FRET probe pYSCS responds to the proteolysis of its α-spectrin calpain cleavage site with an irreversible loss of FRET (Vanderklish *et al.* 2000). Although a portion of the encoded protein localized to post-synaptic densities, the majority of the fluorescence was in the cytoplasm. We found that the fluorescence of the eYFP component of pYSCS exhibited a substantial decrease in intensity when neurons were stimulated with glutamate or underwent DCD. This observation is consistent with quenching of the eYFP FRET acceptor by a decrease in pH or an increase of $[Cl^-]$ in glutamate-stimulated neurons (Wu *et al.* 1999;Zhang *et al.* 2002;Slemmer *et al.* 2004). In addition to the cross talk between CFP, YFP and FRET channels, fluorescence of Fura-6F significantly contributed to the CFP and FRET images and the CFP and the YFP to the Fura-6F emission in brightly expressing cells. Therefore the measured fluorescence intensities (*F*) were first spectrally (linearly) unmixed (resulting fluorescence intensities specific for each fluorophore *F'*, see Supplementary Methods). $[Ca^{2+}]_c$ is given as the ratio of unmixed Fura-6F intensities ($R_{Fura6F}=F'_{340}/F'_{380}$). Because of saturating concentrations of intracellular calcium after DCD *RFura6F* was not calibrated to show micromolarity. To correct for the loss of eYFP fluorescence yield, a three wavelength-corrected FRET ratio calculation was used in place of a simple emission ratio that was used earlier in fixed cells, where ionic effects did not contribute (Vanderklish *et al.* 2000). This was expressed as $FRET = F'_{FRET} / \sqrt{F'_{CFP} F'_{YFP}}$. Image analysis was performed in custom software developed in Delphi 2009 (Embarcadero Technologies, San Francisco, CA).

Cross-correlation analysis

The kinetics of corrected FRET ratio and Fura-6F ratio were heterogeneous among neurons. To provide a relative comparison of changes in these signals, temporal cross-correlation of differentiated signals was calculated. Because cross-correlalograms show the relative relationship of compared signals in time, the cell-by-cell heterogeneity cancels and the mean of the correlalograms can be calculated. Calculations were performed using standard functions of Mathematica 5.2 (Wolfram Research, Champaign, IL), see Supplementary Methods. Cross-correlalograms provide the following information when `trace 1' (FRET) is

compared to `trace 2' (Fura-6F): changes in trace 1 and 2 occurring at the same time in the same direction (increase or decrease) are indicated by a positive peak at zero time. Changes occurring at the same time in the opposite direction (for instance decrease in 1 and increase in 2) are indicated by a negative peak. When the change in 1 occurs after the change in 2, the peak of the cross-correlation diagram shifts to a positive time lag.

Initial changes of ion concentrations during glutamate exposure

Wide-field image acquisition was performed as stated above, but by Metafluor 6.3 (Molecular Devices). For imaging Fura-4F, an ND 1.5 attenuator, 4×4 binning, and 400 and 200 ms exposure times were used for the 340 and 380 nm excitations, respectively, at a four seconds image acquisition interval. For imaging SBFI plus PMPI, an ND 0.5 attenuator, 4×4 binning, and 300, 100 and 30 ms exposure times were used for SBFI 340, 380 nm and PMPI 500 nm excitations, respectively. There was no measurable cross-talk between SBFI and PMPI emissions.

Fura-4F ratios ($R=F_{340}/F_{380}$) were calibrated to micromolarity using the $[Ca^{2+}]=K_d\times((R-R_{min})/(R_{max}-R))\times F_{free380}/F_{sat380}$ equation (Grynkiewicz *et al.* 1985). Cells were exposed to zero and saturating (10 mM free) $[Ca^{2+}]$, yielding the minimal fluorescence ratio (R_{min}) plus the intensity of the Ca^{2+}-unbound Fura-4F at the 380 nm excitation ($F_{free380}$) and the maximal ratio (R_{max}) plus the intensity of Ca^{2+}-saturated Fura-4F at the 380 nm excitation (F_{sat380}), respectively. To calculate the $F_{free380}/F_{sat380}$ ratio, cell swelling and dye leakage were compensated by normalization of $F_{free380}$ and F_{sat380} with the isosbestic fluorescence intensity calculated for the matching time points (Gerencser and Nicholls 2008). To obtain the above parameters, the imaging medium was replaced with `intracellular medium' containing (in mM): 123 KCl, 12.4 NaCl, 20 KOH, 10 EGTA, 20 PIPES with, and then, without 20 mM $CaCl_2$ (pH 7.2) and supplemented with 20 μM 4Br-A23187 (AG Scientific, San Diego), 10 μM nigericin, 10 μM monensin, and 1 μM antimycin A to establish complete equilibration of $[Ca^{2+}]$ and pH (Gerencser and Adam-Vizi 2005). The K_d of Fura-4F was taken as 770 nM according to the manufacturer. SBFI was calibrated similarly to Fura-4F, but parameters were obtained by a three-point calibration at rest (where $[Na^+]_c$ was 11.4±0.3 mM; n=3; determined in separate experiments), after complete equilibration with the imaging medium ($[Na^+]_e$ =136 mM) in the presence of gramicidin (10 μg/ml), and after wash with nominally Na^+-free (choline chloride substituted) medium. This calibration provided R_{min}, R_{max} and $K_d\times F_{free380}/F_{sat380}$ from ratios measured at the above conditions (see Supplementary Methods). The PMPI fluorescence was converted to millivolts by a dynamic, Nernstian, compartment model-based calibration technique (see Supplementary Methods). The calibration was based on the measurement of PMPI fluorescence at K^+-equilibrium potential (-80.4 mV) in the presence of valinomycin (1 μM; a K^+-selective ionophore) and oligomycin (2 μg/ml) (at $[K^+]_e$=3.9 mM and $[K^+]_c$=79.1±1.4 mM; n=3), and at zero $\Delta\Psi_P$ after addition of gramicidin (10 μg/ml; a K^+-Na^+-ionophore). The resting $\Delta\Psi_P$ was -59.9±1.2 mV (n=3 exps.). For the glutamate-treatment experiments the resting and zero potentials were used as calibration points, and the gramicidin treatment was common calibration step with the $[Na^+]$=136 mM point of the SBFI calibration. This procedure was performed at the end of each experiment and calculations were done cell-by-cell in Mathematica 5.2. The means ± SE of the calibrated values are shown.

Calculation of the Gibbs free energy (ΔG) of the NCX

To calculate ΔG, the measured mean $[Ca^{2+}]$, $[Na^+]_c$ and $\Delta\Psi_P$ in addition to $[Na^+]_e$=136 mM and $[Ca^{2+}]_e$=1.3 mM were used:

$$\Delta G = RT\log\frac{\left[Ca^{2+}\right]_e[Na^+]_c^n}{\left[Ca^{2+}\right]_c[Na^+]_e^n} + (2-n)F\Delta\Psi_p \qquad \text{Eq. 1}$$

In Eq. 1 R=8.3 J mol^{-1} K^{-1} (gas constant); T=310 K (temperature); F=96485 J mol^{-1} V^{-1} (Faraday constant), n is the exchange ratio and the $\Delta\Psi_P$ is given in negative volts. The exchange ratio of Na^+:Ca^{2+} is known to be near to 3:1, but higher, non-integer values were also often reported (Blaustein and Lederer 1999;Bers and Ginsburg 2007). In resting neurons the NCX is considered to be in equilibrium, thus its ΔG is zero. In our case this was satisfied with n=3.1, therefore this value was used to calculate ΔG. The error of ΔG was calculated by propagating the SE of the measured parameters though the calculations (Gerencser *et al.* 2008).

Imaging the time-course of DCD, membrane potential changes, and cell death

Imaging was performed using an LSM 5 Pascal laser scanning confocal system (Carl Zeiss AG, Oberkochen, Germany) with a 20x NEOFLUAR NA0.5 air objective lens in room air in a temperature-controlled enclosure at 37°C. For simultaneous imaging of DCD and membrane potential changes, neurons in 8-well Lab-Tek chambers were loaded with Fluo-4FF-AM (0.5 μM) and $TMRM^+$ (5 nM) in the presence of tetraphenylboron (1 μM) in imaging medium for 60-90 minutes at 37°C. Fluo-4FF and $TMRM^+$ were simultaneously excited at 488 and 543 nm and emissions were monitored using a 505-530 nm and a 560LP filter, respectively. There was no measurable cross-talk between the emissions of Fluo-4FF and $TMRM^+$.

Fluorescent time-courses from four independent wells of the Lab-Tek dish were acquired in parallel using the Multi Time Lapse Module, recording a time point for each well at every 4 min. Neurons displaying $TMRM^+$ fluorescence that was lost upon glutamate stimulation (signifying $\Delta\Psi_P$ depolarization) were selected for analysis.

For cell viability experiments, membrane potential polarization, apoptosis, and cell death were determined in parallel using $TMRM^+$, the early plasma membrane permeabilization marker Yo-Pro-1, and the necrosis marker propidium iodide (PI), respectively. The dyes were simultaneously excited at 488 and 543 nm, and emissions were detected at 505-530 nm for Yo-Pro-1, at 560-615 nm for $TMRM^+$ and at 608-683 nm for PI. The PI staining was punctate and distinctly nuclear while $TMRM^+$ fluorescence was cytoplasmic, enabling us to use these dyes in concert despite partial spectral overlap. Neurons pre-treated with 10 μM calpeptin or vehicle for 30 min in imaging buffer were subsequently exposed to glutamate. After 30 min of glutamate or vehicle treatment, imaging buffer was removed and replaced with previously saved culture medium diluted with fresh medium at 1:1. This medium was supplemented with HEPES (20 mM) to buffer pH and MK-801 (10 μM) and 2,3-dihydroxy-6-nitro-7-sulfamoylbenzo[f]quinoxaline-2,3-dione (NBQX; 10 μM) to block NMDA and AMPA receptors, respectively. The number of healthy neurons defined as $TMRM^+$ positive, PI negative, the number of apoptotic neurons defined as Yo-Pro-1 positive, PI negative, and the number of necrotic neurons defined by PI positive nuclear staining were counted at 0, 4, 8, 12, and 20 hours following glutamate treatment.

Immunoblot analysis

Following the acquisition of fluorescent time-courses, imaging buffer was aspirated from the wells and neurons were lysed by scraping in 50 μl of radioimmunoprecipation assay buffer consisting of 150 mM NaCl, 50 mM Tris, 1 mM EDTA, 1 mM EGTA, 1% Triton X-100,

0.5% sodium deoxycholate, 0.1% sodium dodecylsulfate, and 1× Halt Protease Inhibitor Cocktail (Pierce Biotechnology, Rockford, IL) or Protease Inhibitor Cocktail Set III (EMD Biosciences), pH 7.4. Solubilization of membrane proteins was enhanced by three freeze-thaw cycles followed by incubation in SDS-PAGE sample buffer containing 5% β-mercaptoethanol for 30 min at 37° C. Seven to 20 μg of neuronal protein was separated on 4-20% Tris-HEPES gradient gels (ISC BioExpress, Kaysville, UT) by SDS-PAGE and transferred to PVDF membranes (Bio-Rad, Hercules, CA). Immunodetection was performed by standard procedures using SuperSignal West Pico or West Fempto enhanced chemiluminescence substrates (Pierce Biotechnology) and the following dilutions of primary antibodies: 1:500 anti-α-spectrin (0.2 μg/ml), 1:5000 anti-β-actin, 1:1000 anti-NCX3.

Statistical analysis

The incidence and time to DCD in the absence and presence of calpain inhibitor was analyzed for statistical differences using paired Student's t-test comparing the same-day controls. Numbers of neurons exhibiting RCE or recovery were compared with Fisher's exact test in GraphPad Prism 4 (GraphPad Software, Inc., San Diego, CA). To examine whether calpeptin modified the effect of glutamate on $TMRM^+$ or propidium iodide fluorescence, logistic regression analysis was used (see Supplemental Methods). Averages are represented in the text as mean ± SE.

RESULTS

Real-time visualization of calpain activation and DCD

Cytoplasmic calcium changes and calpain activity were monitored in single cells simultaneously with wide field microscopy using the low affinity Ca^{2+} dye Fura-6F (Fig. 1a) and the FRET-based, genetically encoded calpain sensor pYSCS (Fig. 1b), respectively. Cleavage of the pYSCS-encoded protein within the α-spectrin sequence targeted by calpain is expected to trigger an irreversible loss of the FRET between the CFP FRET donor and the YFP FRET acceptor (Vanderklish *et al.* 2000). Cortical cultures were pre-treated with calpeptin (10 μM) or vehicle (DMSO 1:2000) for 30 min and then exposed to glutamate (100 μM; with 10 μM glycine in the absence of Mg^{2+}). Calpeptin (or vehicle) and glutamate were present for the duration of the experiment.

Glutamate evoked a small initial increase of intracellular calcium, as monitored by the Fura-6F ratio over the soma (Fig. 1c-d, black trace). This small calcium increase was followed by delayed calcium deregulation at 5-30 minutes (red pseudocolor in Fig. 1aii and iii). The initial response of the calpain sensor to glutamate was a 14.1 ± 0.8% drop in the amount of FRET in the soma (compared to the baseline; n=58, Fig. 1c, red trace) that was not inhibited by calpeptin (15.2 ± 0.9% n=59). Moreover, in the presence of calpeptin this initial decrease in FRET spontaneously reversed, excluding the possibility that this drop was due to irreversible cleavage of the sensor by calpain (Fig. 1d, red trace; bii). Shortly before DCD the FRET exhibited another calpeptin-insensitive and reversible decrease (Fig. 1c,d, open arrows; see also analysis below). The only *calpeptin-sensitive*, irreversible, `major drop of FRET' (to 37 ± 3% below baseline; n=23) likely to reflect calpain activation occurred long after DCD (Fig. 1c red arrow; Biii, cells b and c). Forty-four of the 58 vehicle pre-treated cells underwent DCD (at 20 ± 3 min after addition of glutamate), and 23 of these also exhibited `calpain activation' typical to that denoted by the red arrow in Fig. 1c. No such change in FRET occurred in cells that did not undergo DCD. We observed only 2 cells with similar FRET characteristics in 49 calpeptin pre-treated neurons undergoing DCD.

Pairs of boxes in Fig. 1e depict the time to DCD and the time to `calpain activation' (relative to glutamate addition) for individual neurons. Pairs connected by lines with a positive

(upward) slope indicate neurons exhibiting `calpain activation' subsequent to DCD. Of note, `calpain activation' was objectively defined as the steepest decrease in FRET beyond a threshold using a computer algorithm. In a few cells (negatively sloped lines in Fig. 1e) the small second drop (Fig. 1c,d, open arrows) was categorized as `calpain activation' by the criterion of steepest decrease. Cells that exhibited DCD but no `calpain activation' during the measured time-frame are shown by triangles. The mean lag time between DCD and calpain activation was 39 ± 5 min (n=23).

The relationship between DCD (increase of Fura-6F ratio) and calpain activation (decrease of pYSCS FRET) was also quantified by calculation of temporal cross-correlation of differentiated signals (Fig. 1f,g). The only marked change in the Fura-6F ratio in the 5-120 min time window after glutamate addition was the increase corresponding to DCD. In contrast the FRET signal typically exhibited multiple drops. In the cross-correlalograms Fig. 1f,g, negative peaks mark changes in the two signals in opposite directions (see Methods). Both control and calpeptin treated cross-correlalograms (Fig. 1f,g) indicate a drop of the FRET signal shortly before DCD (open arrows) that corresponds to the reversible, calpeptin-insensitive decrease in FRET. Importantly, the mean cross-correlalogram in vehicle control-treated neurons (Fig. 1f, solid arrow) has a second negative peak at +39 min that is not present in calpeptin pre-treated cells (Fig. 1g). This calpeptin-sensitive negative peak indicates calpain activation average 39 minutes after DCD, confirming the `binary' calculations of Fig. 1e. The incidence and onset of DCD in pYSCS-transfected neurons was not significantly different in calpeptin-treated cultures; 49 of 59 neurons pre-treated with calpeptin underwent DCD (at 15 ± 3 min, n=49) compared to 44 of 58 (at 20 ± 3 min, n=44) pre-treated with the vehicle control.

A possible spatial heterogeneity of glutamate-triggered calpain activation was also investigated in FRET images (Fig. 1bi-iii). Detectable calpain activation (defined as the `major drop of FRET') occurred after dendrites formed injury-related varicosities (Fig. 1bii), and happened simultaneously in the soma and along the dendrites (e.g. Fig. 1biii and Supplementary Movie 1). However, the possibility of an earlier, local activation of calpain prior to DCD cannot be fully excluded by using pYSCS, because of the large calpeptin-insensitive changes as well as the small true FRET signal compared to the noise amplified by the spectral and FRET corrections.

Our imaging experiments were conducted with neurons cultured for 11-14 DIV at 3% O_2, physiologically relevant to the average 2-4% O_2 (15-30 mM Torr) that was measured in the rat cortex (Grote *et al.* 1996). Because much of the literature on glutamate excitotoxicity investigates neurons cultured at 95% air/5% CO_2 (~20% O_2), we repeated the Fura-6F pYSCS imaging experiments on cortical cultures grown in parallel at 20% O_2. A slightly higher incidence of DCD during the measurement period was observed in neurons grown at 20% O_2 (37 deregulating neurons of 39 total cells) compared to those grown at 3% O_2 (44 of 58). However the properties of calpain activation were almost identical, with 18 of the 37 deregulating neurons showing calpain activation with a 46 ± 4 min delay. None of the 20% O_2-cultured neurons pre-treated with calpeptin displayed the secondary loss of FRET that we associated with calpain activation.

To exclude the possibility that the calpain FRET sensor either influenced the onset of DCD or occluded an effect of calpeptin on DCD onset, we also quantified DCD in the untransfected cell population for the same experiments. As with pYSCS-transfected neurons, calpeptin did not delay the onset of DCD. In contrast, after analyzing a large number of cells we detected a slight but significant increase in the incidence of DCD following 60 minutes of glutamate exposure in calpeptin-treated neurons (Table 1). Similar results were obtained with neurons cultured at 20% O_2.

Independent evaluation of the effect of calpeptin on DCD and calpain inhibition

To additionally confirm that calpeptin does not inhibit DCD, we imaged DCD using a different low affinity calcium indicator (Fluo-4FF; K_d~9.7 μM) in conjunction with the membrane potential sensitive dye $TMRM^+$. Fluo-4FF undergoes a marked increase in fluorescence once calcium homeostasis is lost (Fig 2b, arrows) but is relatively insensitive to calcium increases (~1 μM) mediated by the NMDA receptor (Fig. 2b, arrowhead) (Vesce *et al.* 2004). Prior to glutamate addition, neurons displayed little Fluo-4FF fluorescence and a mitochondrial pattern of $TMRM^+$ fluorescence, indicative of healthy cells with polarized plasma and mitochondrial membrane potentials (Fig 2a). Following glutamate addition, $TMRM^+$ fluorescence was lost and neurons exhibited a stochastic and dramatic rise in Fluo-4FF fluorescence (Fig 2b and c). Under our conditions where the concentration of $TMRM^+$ is insufficient to result in mitochondrial matrix quenching, the drop of $TMRM^+$ signal in response to glutamate primarily reflects plasma membrane potential depolarization (Nicholls 2006) and was used to unambiguously identify neurons responding to glutamate.

Primary cortical neurons lost calcium homeostasis following 100 μM glutamate exposure with a DCD incidence and onset that was not significantly different in the absence or presence of calpeptin. 109 of 110 neurons pre-treated with calpeptin underwent DCD by 60 min (at 18 ± 4 min; n=4) compared to 106 of 107 pre-treated with the vehicle control (at 15 ± 2 min; n=4). Intracellular calcium responses in individual cells (c-d) and averaged Fluo-4FF responses (e) from a representative experiment are depicted in Fig. 2. In some experiments, the calcium ionophore ionomycin (5 μM) was added after the large Fluo-4FF increase associated with DCD. Neurons displaying high Fluo-4FF fluorescence demonstrated no further increase upon ionomycin addition, confirming that DCD had occurred in these cells.

Analysis of α-spectrin and NCX3 cleavage in glutamate-treated cortical neurons

While the calpain FRET sensor experiments suggested that calpeptin was an effective calpain inhibitor, it was important to obtain independent confirmation of intracellular calpain activation and the efficacy of calpain inhibition in our paradigm. Therefore cortical neurons incubated with glutamate for 1.5 hrs in the presence and absence of calpeptin were harvested following calcium imaging and subjected to immunoblot analysis for the canonical calpain substrate α-spectrin. Consistent with the proteolysis of the α-spectrin-based calpain FRET sensor, we observed glutamate-induced processing of α-spectrin that was inhibited by calpeptin (Fig. 3). Densiometry indicated that calpeptin inhibited the appearance of the α-spectrin breakdown product by >90%. Thus, calpeptin was an effective inhibitor of calpain activation in our experiments even though it was not an effective inhibitor of DCD.

In contrast to α-spectrin, a decrease in full-length NCX3 was not observed (Fig. 3). The 58-60 kD cleavage products reported in glutamate-treated cerebellar granule neurons (Bano *et al.* 2005) were barely detectable in cortical neurons relative to full-length NCX3 following 1.5 hrs of glutamate exposure (≥1 hr of deregulated calcium for most cells). It was therefore unlikely that NCX3 cleavage could account for DCD in this neuronal population.

Testing the effect of calpeptin on reversible calcium elevations (RCE)

Cortical neurons were exposed to glutamate (100 μM), plus glycine (10 μM) in the absence of Mg^{2+} for 12 min. This was followed by application of the NMDA and AMPA receptor antagonists MK801 (10 μM) and NBQX (10 μM), respectively, to conclude the glutamate stimulus. Nearly half of neurons maintained calcium homeostasis during and following the 12 min of glutamate receptor stimulation, i.e. no large amplitude increase in Fluo-4FF fluorescence was observed (Fig 4a). These cells recovered a mitochondrial pattern of

$TMRM^+$ fluorescence following the addition of glutamate receptor antagonists and did not undergo DCD during the subsequent 3 hrs. A small population of cells exhibited irreversible DCD (Fig. 4b). Numbers of neurons exhibiting each typical behavior are summarized in Fig. 4c.

A substantial fraction of neurons underwent a large DCD-like calcium elevation in response to glutamate that could be reversed following cessation of the stimulation (Fig. 4e-h and Supplemental Movie 3). These reversible calcium elevations (RCE) were hallmarked by maintained high $[Ca^{2+}]_c$ during and often after glutamatergic stimulation followed by recovery of calcium homeostasis at a later time point. Recovery was either sustained (Fig. 4e,f) or followed by DCD (Fig. 4g,h). Some of the cells experienced multiple RCE events prior to DCD (Fig. 4h). $TMRM^+$ fluorescence was restored with fast (Fig. 4e) or slow (Fig. 4f) kinetics following the recovery of calcium homeostasis. However, all neurons that failed to recover $TMRM^+$ fluorescence following RCE later displayed DCD.

Although cytoplasmic calpain activation became measurable only after a sustained period of DCD, we hypothesized that localized calpain activity below the threshold for detection might be important for converting the DCD-like calcium elevation from a reversible to an irreversible process. Thus, we tested whether addition of calpeptin changed the frequency of RCE following transient glutamate receptor stimulation and/or improved recovery from RCE. Calpeptin (10 μM, given together with MK801 and NBQX at the conclusion of glutamate receptor stimulation) failed to affect the outcome of the glutamate treatment (Fig. 4c and d).

Evaluation of the chemically distinct calpain inhibitor PD150606

To support the hypothesis that an inhibitory effect of calpeptin on DCD (or RCE) was not masked by non-specific targets, we also tested the chemically unrelated calpain inhibitor PD150606 for protection against DCD. This compound interferes with the calcium binding site rather than the active site of the protease, inhibits purified μ-calpain and m-calpain in the nanomolar range (K_i = 210 nM and 370 nM, respectively), and attenuates α-spectrin breakdown at 1-10 μM in intact cells (Wang *et al.* 1996). As with calpeptin, 10 μM PD150606 did not decrease the incidence of DCD relative to vehicle treated cultures after 60 min of glutamate treatment although the incidence was slightly reduced at 20 min (only significant for 20% O_2 cultures, Table 1). However, increasing PD150606 to 50 μM, a concentration not specific for calpains (Wang *et al.* 1996;Van den *et al.* 2002), resulted in significant protection of neurons at both 20 and 60 min (Table 1).

To determine whether calpain inhibition was a plausable mechanism for its protective action, we assessed the ability of PD150606 to inhibit α-spectrin breakdown. In contrast to the nearly complete inhibition of α-spectrin cleavage by calpeptin, PD150606 even at 50 μM attenuated α-spectrin breakdown by only ~35% (n=3; Fig. 5). This modest inhibition of calpain activity was unlikely to account for the potent protection of 50 μM PD150606 against DCD since the >90% inhibition of calpain proteolysis by calpeptin was without effect.

The effect of calpeptin on cell death

Although calpain activity was not required for DCD or recovery from RCE in response to 100 μM glutamate, it remained possible that the late calpain activation occurring ~40 min after DCD onset was necessary for the efficient execution of cell death. To address this possibility, we measured the number of healthy, apoptotic, and necrotic neurons at 4, 8, 12, or 20 hours after a 30 min excitotoxic glutamate stimulus with or without calpeptin pre-treatment (Fig. 6). PD150606 was not evaluated in this assay due to its limited efficacy as a

calpain inhibitor (Fig. 5) and its ability to inhibit multiple calcium-dependent pathways (e.g. Ca^{2+}-calmodulin dependent calcineurin activity (Wang *et al.* 1996)). Healthy neurons excluded the apoptosis marker Yo-Pro-1 and the necrosis marker propidium iodide (PI) from the nucleus and displayed mitochondrial (cytoplasmic) $TMRM^+$ fluorescence. Apoptotic neurons were defined as cells with nuclear Yo-Pro-1 fluorescence that excluded PI. Neurons exhibiting nuclear PI fluorescence without cytoplasmic $TMRM^+$ fluorescence were considered necrotic.

We observed no significant effect of calpeptin on the number of healthy or necrotic neurons at any of the time points measured, as assessed by logistic regression analysis (Fig. 6). Apoptotic neurons were not observed at any time point. We also observed no significant effect of calpeptin in parallel assays using cortical neurons cultured at 20% O_2 (data not shown). Thus, cell death in response to 100 μM glutamate occurred with a normal time course in the presence of effective calpain inhibition.

Assessing NCX function in acute glutamate excitotoxicity

Finally, although we were unable to detect a significant decrease of full-length NCX3 protein in cortical neurons exposed to glutamate (Fig. 3), it remained possible that a functional loss of NCX activity influenced DCD onset. To assess the workload on the NCX in glutamate-treated cortical neurons, the initial, glutamate-evoked rise of $[Ca^{2+}]_c$ and $[Na^+]_c$ depolarization of the plasma membrane potential ($\Delta\Psi_P$) were measured using wide-field fluorescence microscopy. To resolve the initial effects and reversibility of the glutamate treatment, a perfusion system was used to deliver glutamate (100 μM) plus glycine (10 μM) and to wash out Mg^{2+}.

Fig. 7a-c shows the transients of $[Ca^{2+}]_c$, $[Na^+]_c$ and $\Delta\Psi_P$ evoked by a 160 s glutamate exposure. Remarkably, the almost instantaneous rise of $[Ca^{2+}]_c$ (a) and depolarization of the plasma membrane to +10 mV (c) was paralleled by a gradual, high amplitude rise of $[Na^+]$ (b). The large changes in the $[Na^+]_c$ and $\Delta\Psi_P$ suggested that a forward mode of Na^+-Ca^{2+} exchange was not feasible under these circumstances. To quantify the thermodynamic driving force on the NCX, we calculated the ΔG of the forward reaction (Ca^{2+} extrusion). The data in Fig. 7d indicate that after addition of glutamate the NCX operated in forward mode for only a very short initial period, during the initial rise of $[Ca^{2+}]_c$ and before the gross rise of $[Na^+]_c$. From this time point (<10 sec after glutamate application) the NCX reversed, favoring Ca^{2+} entry, and remained reversed for the entire duration of the experiment (ΔG>0). While washing out glutamate led to quick re- (and hyper-) polarization of the plasma membrane and close-to-baseline recovery of $[Ca^{2+}]_c$ (Fig. 7a and c), the elevated $[Na^+]_c$ (Fig. 7b) supported a maintained reversal of the NCX (Fig. 7d). $[Ca^{2+}]_c$ did not recover completely to baseline until the end of the experiment likely due to Ca^{2+} influx via the maintained reversal of the NCX (Fig. 7a).

To confirm that the NCX works in reverse during the glutamate-triggered Ca^{2+} plateau, the reverse mode-selective NCX inhibitor KB-R7943 (10 μM) was added on top of the glutamate treatment (Fig. 7e). A decrease in $[Ca^{2+}]_c$ was observed upon addition of KB-R7943. This decrease suggested that Ca^{2+} entry through reversed NCX contributed to the glutamate-triggered Ca^{2+} plateau. The Ca^{2+} channel blocker nifedipine (1 μM) was present in this experiment to exclude the possibility that the effect of KB-R7943 was due to the inhibition of voltage-dependent Ca^{2+} channels (Dietz *et al.* 2007). Remarkably, blocking NCX activity with KB-R7943 decreased the incidence of DCD during a 20 or 60 min glutamate exposure (Table 1). Thus any inhibition of plasmalemmal NCX function by calpain or other mechanisms would delay rather than promote the induction of DCD in cortical neurons.

DISCUSSION

Calpain proteases play an undisputed but incompletely characterized role in neuronal injury. Calpain inhibitors are protective to varying degrees in animal models of stroke (Bartus *et al.* 1994;Markgraf *et al.* 1998;Tsubokawa *et al.* 2006), traumatic brain injury (Saatman *et al.* 1996;Buki *et al.* 2003;Ai *et al.* 2007), Alzheimer's disease (Trinchese *et al.* 2008), and Parkinson's disease (Crocker *et al.* 2003). Additionally, calpain-generated α-spectrin breakdown products in cerebrospinal fluid are associated with traumatic brain injury severity in humans (Pineda *et al.* 2007). However, despite the early promise of calpain inhibitors, data on long-term outcome in animal studies remains sparse and successful clinical studies in humans have yet to materialize. It is clear that multiple cell death mechanisms contribute to the spatiotemporal profile of neuronal loss *in vivo* and a better understanding of the participation of calpain proteases in the pathogenesis of different injury paradigms is required for the development of targeted treatments. In this study we set out to: 1) identify whether the major activation of calpain proteases in the cytoplasm occurs up or downstream of glutamate-induced intracellular calcium deregulation and 2) determine whether calpain activity is required for excitotoxic calcium deregulation or cell death in cortical neurons.

Using a genetically encoded calpain sensor, we demonstrated that somal cytoplasmic calpain activity becomes detectable via fluorescent substrate within a very narrowly defined time window at approximately 40 min after the onset of DCD (Fig. 1). Once initiated, cleavage of the FRET sensor progressed at a constant rate until the loss of FRET was complete (Fig. 1c), suggesting that this event represented `major' unchecked calpain activation.

The mechanisms of calpain activation in intact neurons are incompletely understood. *In vitro*, both μ-calpain (3-50 μM) and m-calpain (0.4-0.8 mM) require supra-physiological calcium concentrations for activation (Goll *et al.* 2003). Furthermore, the constitutive expression of an endogenous inhibitor protein, calpastatin, is predicted to limit calpain activity in response to transient pulses of high calcium while ultimately succumbing to proteolysis only if elevated calcium is sustained (Goll *et al.* 2003;Rami 2003). Thus, unchecked calpain activation in neurons is expected only after a period of prolonged calcium deregulation. Our data in Fig. 1 are consistent with a model where the calpastatin-mediated check on calpain activity is relieved following 40 min of sustained DCD, allowing unimpeded calpain proteolysis of cytoplasmic substrates to progress. Because calpain is reportedly sequestered in subcellular membrane fractions including mitochondria (Hewitt *et al.* 1998;Garcia *et al.* 2005;Ozaki *et al.* 2007;Kar *et al.* 2008), an alternative possibility is that the delayed but distinct cytoplasmic calpain activation with respect to DCD represents a subcellular translocation event that brings active calpain in contact with the fluorescent sensor.

Spectrin breakdown products and a decrease in FRET were reported in pYSCS-transfected hippocampal neuron dendritic spines within 5 min of glutamate treatment (Vanderklish *et al.* 2000). In our experiments, glutamate treatment of cortical neurons caused an initial calpain-independent, reversible decrease in FRET, suggesting that conformational changes of the probe affect FRET efficiency. While the spectral unmixing and three-wavelength FRET calculation avoided errors originating from spectral bleed-through and variations of FRET acceptor fluorescence yield, these calculations also decreased signal-to-noise ratio. Due to the high calpain-insensitive background we cannot confirm or reject the possibility of localized calpain activation (e.g. in sub-plasma membrane regions) prior to DCD. However, our data do not support a generalized early increase in calpain activity.

The literature on whether calpain activation causatively contributes to glutamate receptor-mediated cell death is inconsistent. Early studies found that calpain activity was not required

for glutamate excitotoxicity in cerebellar granule (Manev *et al.* 1991) or hippocampal (Adamec *et al.* 1998) neurons, while neuroprotection by calpain inhibitors was reported by others in response to glutamate, kainate, or NMDA (Brorson *et al.* 1995;Rami *et al.* 1997;Lankiewicz *et al.* 2000;Tremblay *et al.* 2000;Araujo *et al.* 2004;Bano *et al.* 2005;Hou *et al.* 2006;Araujo *et al.* 2007;Beart *et al.* 2007;Bevers *et al.* 2009). Although few of these studies addressed the mechanistic involvement of calpains in death, one found that calpain inhibition delayed the late stages of AMPA-induced cortical neuron death (PI positivity) without preventing early hallmarks of mitochondrial dysfunction (decreased dehydrogenase activity, cytochrome *c* release) (Beart *et al.* 2007). However, another found that overexpression of calpastatin inhibited DCD in cerebellar granule neurons (Bano *et al.* 2005), suggesting an upstream role for calpain involvement in excitotoxic cell death.

Here we found that calpeptin effectively inhibited calpain-mediated α-spectrin breakdown (Fig 3) without decreasing the incidence or onset of glutamate-induced DCD (Fig. 2, Table 1). In fact, a small but significant increase in the incidence of DCD was detected when large numbers of neurons were considered, possibly due to inhibition of local calpain processing of NMDA NR2 subunits (Wu *et al.* 2005). Calpeptin was also unable to improve the rate of sustained $[Ca^{2+}]_c$ recovery following glutamate-triggered DCD-like reversible calcium elevations (Fig. 4 and Supplemental Movie 3), or protect against necrotic cell death (Fig. 6). Apoptotic death was not observed in the present study. Because calpain inhibition protects against neuronal apoptosis (Ray *et al.* 2006;Cao *et al.* 2007), we hypothesize that the percentage of neurons undergoing apoptosis *vs*. necrosis in response to a given excitotoxic challenge ultimately determines the ability of calpain inhibitors to effectively delay glutamate receptor-related injury.

Our primary findings contrast with a recent report that overexpression of calpastatin inhibits DCD in cerebellar granule neurons by preventing calpain-mediated NCX3 cleavage (Bano *et al.* 2005). The onset of DCD in cerebellar granule neurons is considerably delayed relative to cortical neurons (e.g. compare Fig. 2 to (Bano *et al.* 2005)) and it is possible that different mechanisms (apoptotic vs. necrotic) contribute to injury. The expression of NCX3 relative to NCX1 also differs between cortical and cerebellar granule neurons (Kiedrowski *et al.* 2004). We failed to see the appearance of 58-60 kD NCX3 breakdown products or a degradation of full-length NCX3 in glutamate-treated cortical neurons even after 1.5 hr of continuous glutamate treatment (and ~1 hr after DCD, Fig. 3). The NCX antagonist KB-R7943 delayed rather than shortened the time to DCD (Table 1), suggesting that in our model NCX activity following glutamate exposure was deleterious rather than protective. Calculation of the ΔG for Na^+/Ca^{2+} exchange (Fig. 7) revealed that NCX operates in reverse mode favoring Ca^{2+} entry during glutamate exposure, in agreement with previous reports (Kiedrowski *et al.* 1994;Hoyt *et al.* 1998;Czyz and Kiedrowski 2002;Kiedrowski *et al.* 2004;Araujo *et al.* 2007;Storozhevykh *et al.* 2007). Consistent with reverse mode NCX operation, KB-R7943 acutely decreased intracellular Ca^{2+} when administered after glutamate addition (Fig. 7e). Thus, NCX failure cannot explain the sudden loss of calcium homeostasis in glutamate-exposed cortical neurons although failure of other calcium extrusion pathways (e.g. the PMCA (Pottorf *et al.* 2006)) may contribute.

In summary, our studies for the first time imaged somal calpain activation relative to intracellular calcium changes in live glutamate-treated neurons, revealing the onset of major activity following ~40 min of sustained DCD. Modifications of this technique, particularly ones that reduce pH-sensitive and calpeptin-insensitive changes in fluorescence, should be useful for characterizing calpain activation in less acute models of neuronal injury where calpain inhibitors are protective.

Supplementary Material

Refer to Web version on PubMed Central for supplementary material.

Acknowledgments

We thank Richard Oh for the preparation of primary cortical and hippocampal neurons, Dr. Ken Philipson for generously providing NCX3 antibody, and Dr. Peter Vanderklish for kindly providing the pYSCS plasmid. This work was supported by NIH grants PL1 AG032118 and P30 AG025708 at the Buck Institute and by NIH grant NS054764 to B.M.P.

Abbreviations

AMPA	α-amino-3-hydroxy-5-methylisoxazole-4-propionate
DCD	delayed calcium deregulation
FRET	fluorescence resonance energy transfer
NBQX	2,3-dihydroxy-6-nitro-7-sulfamoyl-benzo[f]quinoxaline-2,3-dione
NCX	sodium-calcium exchanger
NMDA	N-methyl-D-aspartate
$\Delta\Psi_P$	plasma membrane potential
PI	propidium iodide
PMCA	plasma membrane calcium ATPase
PMPI	plasma membrane potential indicator
RCE	reversible calcium elevations
$TMRM^+$	tetramethylrhodamine methyl ester

REFERENCES

Adamec E, Beermann ML, Nixon RA. Calpain I activation in rat hippocampal neurons in culture is NMDA receptor selective and not essential for excitotoxic cell death. Brain Res. Mol. Brain Res. 1998; 54:35–48. [PubMed: 9526039]

Ai J, Liu E, Wang J, Chen Y, Yu J, Baker AJ. Calpain inhibitor MDL-28170 reduces the functional and structural deterioration of corpus callosum following fluid percussion injury. J. Neurotrauma. 2007; 24:960–978. [PubMed: 17600513]

Araujo IM, Carreira BP, Pereira T, Santos PF, Soulet D, Inacio A, Bahr BA, Carvalho AP, Ambrosio AF, Carvalho CM. Changes in calcium dynamics following the reversal of the sodium-calcium exchanger have a key role in AMPA receptor-mediated neurodegeneration via calpain activation in hippocampal neurons. Cell Death Differ. 2007; 14:1635–1646. [PubMed: 17585341]

Araujo IM, Verdasca MJ, Leal EC, Bahr BA, Ambrosio AF, Carvalho AP, Carvalho CM. Early calpain-mediated proteolysis following AMPA receptor activation compromises neuronal survival in cultured hippocampal neurons. jnc. 2004; 91:1322–1331.

Bano D, Young KW, Guerin CJ, Lefeuvre R, Rothwell NJ, Naldini L, Rizzuto R, Carafoli E, Nicotera P. Cleavage of the plasma membrane na(+)/ca(2+) exchanger in excitotoxicity. Cell. 2005; 120:275–285. [PubMed: 15680332]

Bartus RT, Hayward NJ, Elliott PJ, Sawyer SD, Baker KL, Dean RL, Akiyama A, Straub JA, Harbeson SL, Li Z. Calpain inhibitor AK295 protects neurons from focal brain ischemia. Effects of postocclusion intra-arterial administration. Stroke. 1994; 25:2265–2270. [PubMed: 7974554]

Beart PM, Lim ML, Chen B, Diwakarla S, Mercer LD, Cheung NS, Nagley P. Hierarchical recruitment by AMPA but not staurosporine of pro-apoptotic mitochondrial signaling in cultured

cortical neurons: evidence for caspase-dependent/independent cross-talk. jnc. 2007; 103:2408–2427.

Bers DM, Ginsburg KS. Na:Ca stoichiometry and cytosolic Ca-dependent activation of NCX in intact cardiomyocytes. Ann N Y Acad Sci. 2007; 1099:326–338. [PubMed: 17303827]

Bevers MB, Lawrence E, Maronski M, Starr N, Amesquita M, Neumar RW. Knockdown of m-calpain increases survival of primary hippocampal neurons following NMDA excitotoxicity. J Neurochem. 2009; 108:1237–1250. [PubMed: 19141074]

Bevers MB, Neumar RW. Mechanistic role of calpains in postischemic neurodegeneration. J. Cereb. Blood Flow Metab. 2008; 28:655–673. [PubMed: 18073773]

Blaustein MP, Lederer WJ. Sodium/calcium exchange: its physiological implications. Physiol Rev. 1999; 79:763–854. [PubMed: 10390518]

Bolshakov AP, Mikhailova MM, Szabadkai G, Pinelis VG, Brustovetsky N, Rizzuto R, Khodorov BI. Measurements of mitochondrial pH in cultured cortical neurons clarify contribution of mitochondrial pore to the mechanism of glutamate-induced delayed Ca2+ deregulation. cc. 2008; 43:602–614.

Bredesen DE, Rao RV, Mehlen P. Cell death in the nervous system. Nature. 2006; 443:796–802. [PubMed: 17051206]

Brorson JR, Marcuccilli CJ, Miller RJ. Delayed antagonism of calpain reduces excitotoxicity in cultured neurons. Stroke. 1995; 26:1259–1266. [PubMed: 7541574]

Buki A, Farkas O, Doczi T, Povlishock JT. Preinjury administration of the calpain inhibitor MDL-28170 attenuates traumatically induced axonal injury. J. Neurotrauma. 2003; 20:261–268. [PubMed: 12820680]

Cao G, Xing J, Xiao X, Liou AK, Gao Y, Yin XM, Clark RS, Graham SH, Chen J. Critical role of calpain I in mitochondrial release of apoptosis-inducing factor in ischemic neuronal injury. JNS. 2007; 27:9278–9293.

Castilho RF, Hansson O, Ward MW, Budd SL, Nicholls DG. Mitochondrial control of acute glutamate excitotoxicity in cultured cerebellar granule cells. JNS. 1998; 18:10277–10286.

Crocker SJ, Smith PD, Jackson-Lewis V, Lamba WR, Hayley SP, Grimm E, Callaghan SM, Slack RS, Melloni E, Przedborski S, Robertson GS, Anisman H, Merali Z, Park DS. Inhibition of calpains prevents neuronal and behavioral deficits in an MPTP mouse model of Parkinson's disease. JNS. 2003; 23:4081–4091.

Czyz A, Kiedrowski L. In depolarized and glucose-deprived neurons, Na+ influx reverses plasmalemmal K+-dependent and K+-independent Na+/Ca2+ exchangers and contributes to NMDA excitotoxicity. jnc. 2002; 83:1321–1328.

Dietz RM, Kiedrowski L, Shuttleworth CW. Contribution of Na(+)/Ca(2+) exchange to excessive Ca(2+) loading in dendrites and somata of CA1 neurons in acute slice. Hippocampus. 2007; 17:1049–1059. [PubMed: 17598158]

Friedrich P. The intriguing Ca(2+) requirement of calpain activation. Biochem. Biophys. Res. Commun. 2004; 323:1131–1133. [PubMed: 15451413]

Garcia M, Bondada V, Geddes JW. Mitochondrial localization of mu-calpain. Biochem. Biophys. Res. Commun. 2005; 338:1241–1247. [PubMed: 16259951]

Gerencser AA, Adam-Vizi V. Mitochondrial Ca2+ dynamics reveals limited intramitochondrial Ca2+ diffusion. Biophys. J. 2005; 88:698–714. [PubMed: 15501949]

Gerencser AA, Doczi J, Torocsik B, Bossy-Wetzel E, Adam-Vizi V. Mitochondrial swelling measurement in situ by optimized spatial filtering: astrocyte-neuron differences. Biophys. J. 2008; 95:2583–2598. [PubMed: 18424491]

Gerencser AA, Nicholls DG. Measurement of instantaneous velocity vectors of organelle transport: mitochondrial transport and bioenergetics in hippocampal neurons. Biophys. J. 2008; 95:3079–3099. [PubMed: 18757564]

Goll DE, Thompson VF, Li H, Wei W, Cong J. The calpain system. Physiol Rev. 2003; 83:731–801. [PubMed: 12843408]

Grote J, Laue O, Eiring P, Wehler M. Evaluation of brain tissue O2 supply based on results of PO2 measurements with needle and surface microelectrodes. J. Auton. Nerv. Syst. 1996; 57:168–172. [PubMed: 8964943]

Grynkiewicz G, Poenie M, Tsien RY. A new generation of Ca2+ indicators with greatly improved fluorescence properties. J. Biol. Chem. 1985; 260:3440–3450. [PubMed: 3838314]

Guttmann RP, Sokol S, Baker DL, Simpkins KL, Dong Y, Lynch DR. Proteolysis of the N-methyl-d-aspartate receptor by calpain in situ. J. Pharmacol. Exp. Ther. 2002; 302:1023–1030. [PubMed: 12183659]

Hewitt KE, Lesiuk HJ, Tauskela JS, Morley P, Durkin JP. Selective coupling of mu-calpain activation with the NMDA receptor is independent of translocation and autolysis in primary cortical neurons. J. Neurosci. Res. 1998; 54:223–232. [PubMed: 9788281]

Hou ST, Jiang SX, Desbois A, Huang D, Kelly J, Tessier L, Karchewski L, Kappler J. Calpain-cleaved collapsin response mediator protein-3 induces neuronal death after glutamate toxicity and cerebral ischemia. J Neurosci. 2006; 26:2241–2249. [PubMed: 16495451]

Hoyt KR, Arden SR, Aizenman E, Reynolds IJ. Reverse Na+/Ca2+ exchange contributes to glutamate-induced intracellular Ca2+ concentration increases in cultured rat forebrain neurons. MP. 1998; 53:742–749.

Kar P, Chakraborti T, Samanta K, Chakraborti S. Submitochondrial localization of associated mu-calpain and calpastatin. Arch Biochem Biophys. 2008; 470:176–186. [PubMed: 18082616]

Kiedrowski L, Brooker G, Costa E, Wroblewski JT. Glutamate impairs neuronal calcium extrusion while reducing sodium gradient. Neuron. 1994; 12:295–300. [PubMed: 7906528]

Kiedrowski L, Czyz A, Baranauskas G, Li XF, Lytton J. Differential contribution of plasmalemmal Na/Ca exchange isoforms to sodium-dependent calcium influx and NMDA excitotoxicity in depolarized neurons. jnc. 2004; 90:117–128.

Lankiewicz S, Marc LC, Truc BN, Krohn AJ, Poppe M, Cole GM, Saido TC, Prehn JH. Activation of calpain I converts excitotoxic neuron death into a caspase-independent cell death. J. Biol. Chem. 2000; 275:17064–17071. [PubMed: 10828077]

Lee MS, Kwon YT, Li M, Peng J, Friedlander RM, Tsai LH. Neurotoxicity induces cleavage of p35 to p25 by calpain. Nature. 2000; 405:360–364. [PubMed: 10830966]

Lin MT, Beal MF. Mitochondrial dysfunction and oxidative stress in neurodegenerative diseases. Nature. 2006; 443:787–795. [PubMed: 17051205]

Manev H, Favaron M, Siman R, Guidotti A, Costa E. Glutamate neurotoxicity is independent of calpain I inhibition in primary cultures of cerebellar granule cells. jnc. 1991; 57:1288–1295.

Markgraf CG, Velayo NL, Johnson MP, McCarty DR, Medhi S, Koehl JR, Chmielewski PA, Linnik MD. Six-hour window of opportunity for calpain inhibition in focal cerebral ischemia in rats. Stroke. 1998; 29:152–158. [PubMed: 9445345]

Nicholls DG. Mitochondrial dysfunction and glutamate excitotoxicity studied in primary neuronal cultures. Curr. Mol. Med. 2004; 4:149–177. [PubMed: 15032711]

Nicholls DG. Simultaneous monitoring of ionophore- and inhibitor-mediated plasma and mitochondrial membrane potential changes in cultured neurons. J. Biol. Chem. 2006; 281:14864–14874. [PubMed: 16551630]

Ozaki T, Tomita H, Tamai M, Ishiguro S. Characteristics of mitochondrial calpains. J. Biochem. 2007; 142:365–376. [PubMed: 17646173]

Pineda JA, Lewis SB, Valadka AB, Papa L, Hannay HJ, Heaton SC, Demery JA, Liu MC, Aikman JM, Akle V, Brophy GM, Tepas JJ, Wang KK, Robertson CS, Hayes RL. Clinical significance of alphaII-spectrin breakdown products in cerebrospinal fluid after severe traumatic brain injury. J Neurotrauma. 2007; 24:354–366. [PubMed: 17375999]

Polster BM, Basanez G, Etxebarria A, Hardwick JM, Nicholls DG. Calpain I induces cleavage and release of apoptosis-inducing factor from isolated mitochondria. J. Biol. Chem. 2005; 280:6447–6454. [PubMed: 15590628]

Pottorf WJ, Johanns TM, Derrington SM, Strehler EE, Enyedi A, Thayer SA. Glutamate-induced protease-mediated loss of plasma membrane Ca pump activity in rat hippocampal neurons. jnc. 2006; 98:1646–1656.

Rami A. Ischemic neuronal death in the rat hippocampus: the calpain-calpastatin-caspase hypothesis. Neurobiol. Dis. 2003; 13:75–88. [PubMed: 12828932]

Rami A, Ferger D, Krieglstein J. Blockade of calpain proteolytic activity rescues neurons from glutamate excitotoxicity. Neurosci. Res. 1997; 27:93–97. [PubMed: 9089703]

Randall RD, Thayer SA. Glutamate-induced calcium transient triggers delayed calcium overload and neurotoxicity in rat hippocampal neurons. JNS. 1992; 12:1882–1895.

Ray SK, Karmakar S, Nowak MW, Banik NL. Inhibition of calpain and caspase-3 prevented apoptosis and preserved electrophysiological properties of voltage-gated and ligand-gated ion channels in rat primary cortical neurons exposed to glutamate. N. 2006; 139:577–595.

Saatman KE, Murai H, Bartus RT, Smith DH, Hayward NJ, Perri BR, McIntosh TK. Calpain inhibitor AK295 attenuates motor and cognitive deficits following experimental brain injury in the rat. Proc. Natl. Acad. Sci. U. S. A. 1996; 93:3428–3433. [PubMed: 8622952]

Siman R, Noszek JC. Excitatory amino acids activate calpain I and induce structural protein breakdown in vivo. Neuron. 1988; 1:279–287. [PubMed: 2856162]

Simpkins KL, Guttmann RP, Dong Y, Chen Z, Sokol S, Neumar RW, Lynch DR. Selective activation induced cleavage of the NR2B subunit by calpain. JNS. 2003; 23:11322–11331.

Slemmer JE, Matsushita S, De Zeeuw CI, Weber JT, Knopfel T. Glutamate-induced elevations in intracellular chloride concentration in hippocampal cell cultures derived from EYFP-expressing mice. Eur. J. Neurosci. 2004; 19:2915–2922. [PubMed: 15182298]

Springer JE, Azbill RD, Kennedy SE, George J, Geddes JW. Rapid calpain I activation and cytoskeletal protein degradation following traumatic spinal cord injury: attenuation with riluzole pretreatment. jnc. 1997; 69:1592–1600.

Storozhevykh TP, Sorokina EG, Vabnitz AV, Senilova YE, Tukhbatova GR, Pinelis VG. Na+/Ca2+ exchange and regulation of cytoplasmic concentration of calcium in rat cerebellar neurons treated with glutamate. Biochemistry (Mosc.). 2007; 72:750–759. [PubMed: 17680767]

Stout AK, Raphael HM, Kanterewicz BI, Klann E, Reynolds IJ. Glutamate-induced neuron death requires mitochondrial calcium uptake. Nat. Neurosci. 1998; 1:366–373. [PubMed: 10196525]

Tremblay R, Chakravarthy B, Hewitt K, Tauskela J, Morley P, Atkinson T, Durkin JP. Transient NMDA receptor inactivation provides long-term protection to cultured cortical neurons from a variety of death signals. J Neurosci. 2000; 20:7183–7192. [PubMed: 11007874]

Trinchese F, Fa' M, Liu S, Zhang H, Hidalgo A, Schmidt SD, Yamaguchi H, Yoshii N, Mathews PM, Nixon RA, Arancio O. Inhibition of calpains improves memory and synaptic transmission in a mouse model of Alzheimer disease. J Clin Invest. 2008; 118:2796–2807. [PubMed: 18596919]

Tsubokawa T, Yamaguchi-Okada M, Calvert JW, Solaroglu I, Shimamura N, Yata K, Zhang JH. Neurovascular and neuronal protection by E64d after focal cerebral ischemia in rats. J. Neurosci. Res. 2006; 84:832–840. [PubMed: 16802320]

Van den BL, Van DP, Vleminckx V, Van HE, Lemmens G, Missiaen L, Callewaert G, Robberecht W. An alpha-mercaptoacrylic acid derivative (PD150606) inhibits selective motor neuron death via inhibition of kainate-induced Ca2+ influx and not via calpain inhibition. Neuropharmacology. 2002; 42:706–713. [PubMed: 11985829]

Vanderklish PW, Krushel LA, Holst BH, Gally JA, Crossin KL, Edelman GM. Marking synaptic activity in dendritic spines with a calpain substrate exhibiting fluorescence resonance energy transfer. Proc. Natl. Acad. Sci. U. S. A. 2000; 97:2253–2258. [PubMed: 10688895]

Vergun O, Keelan J, Khodorov BI, Duchen MR. Glutamate-induced mitochondrial depolarisation and perturbation of calcium homeostasis in cultured rat hippocampal neurones. J. Physiol. 1999; 519(Pt 2):451–466. [PubMed: 10457062]

Vesce S, Kirk L, Nicholls DG. Relationships between superoxide levels and delayed calcium deregulation in cultured cerebellar granule cells exposed continuously to glutamate. jnc. 2004; 90:683–693.

Wang KK, Nath R, Posner A, Raser KJ, Buroker-Kilgore M, Hajimohammadreza I, Probert AW Jr. Marcoux FW, Ye Q, Takano E, Hatanaka M, Maki M, Caner H, Collins JL, Fergus A, Lee KS, Lunney EA, Hays SJ, Yuen P. An alpha-mercaptoacrylic acid derivative is a selective nonpeptide cell-permeable calpain inhibitor and is neuroprotective. Proc. Natl. Acad. Sci. U. S. A. 1996; 93:6687–6692. [PubMed: 8692879]

Wu HY, Tomizawa K, Oda Y, Wei FY, Lu YF, Matsushita M, Li ST, Moriwaki A, Matsui H. Critical role of calpain-mediated cleavage of calcineurin in excitotoxic neurodegeneration. J. Biol. Chem. 2004; 279:4929–4940. [PubMed: 14627704]

Wu HY, Yuen EY, Lu YF, Matsushita M, Matsui H, Yan Z, Tomizawa K. Regulation of NMDA receptors by calpain in cortical neurons. J. Biol. Chem. 2005

Wu ML, Chen JH, Chen WH, Chen YJ, Chu KC. Novel role of the Ca(2+)-ATPase in NMDA-induced intracellular acidification. Am. J. Physiol. 1999; 277:C717–C727. [PubMed: 10516102]

Xu W, Wong TP, Chery N, Gaertner T, Wang YT, Baudry M. Calpain-Mediated mGluR1alpha Truncation: A Key Step in Excitotoxicity. Neuron. 2007; 53:399–412. [PubMed: 17270736]

Yuen EY, Gu Z, Yan Z. Calpain regulation of AMPA receptor channels in cortical pyramidal neurons. J. Physiol. 2007a; 580:241–254. [PubMed: 17234699]

Yuen EY, Liu W, Yan Z. The phosphorylation state of GluR1 subunits determines the susceptibility of AMPA receptors to calpain cleavage. J. Biol. Chem. 2007b; 282:16434–16440. [PubMed: 17428797]

Zhang J, Campbell RE, Ting AY, Tsien RY. Creating new fluorescent probes for cell biology. Nat. Rev. Mol. Cell Biol. 2002; 3:906–918. [PubMed: 12461557]

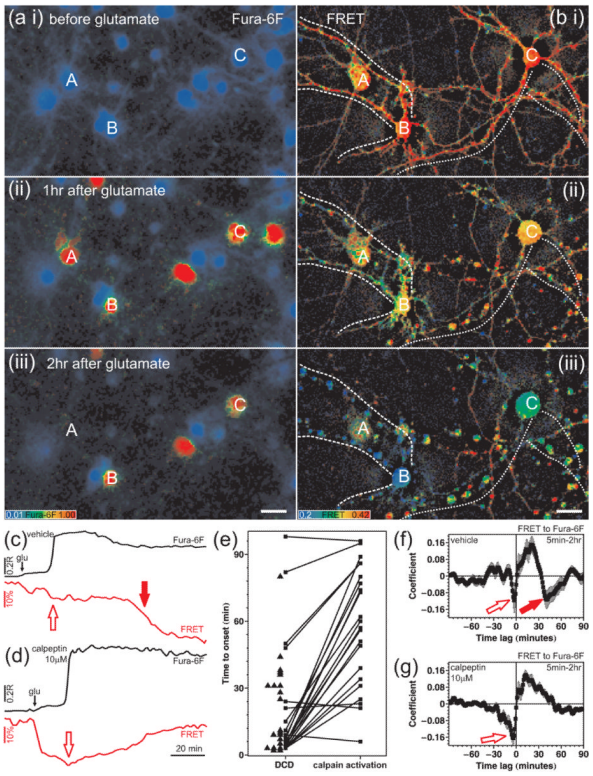

Fig. 1. The temporal relationship of DCD and calpain activation

Cortical cultures expressing the calpain sensor pYSCS were wide-field time lapse imaged during continuous exposure to glutamate. (a) Fura-6F pseudo-colored ratio images. A-C identify three cells expressing pYSCS in (b). Cells not appearing in (a iii; e.g. A) underwent lysis. (b) Spectrally unmixed, aligned, corrected pYSCS FRET ratio images gated with the dehazed (high pass filtered) YFP acceptor fluorescence image. Dashed and dotted lines follow dendrites of cell B and cell C, respectively. Scale bars, 20 μm. (c-d) Representative pairs of Fura-6F ratio (R; black) and corrected FRET ratio (% of baseline; red) traces from a vehicle (c) and a calpeptin (d; 10 μM, 30 min) pre-treated neuron. Open red arrows indicate a DCD-related, but calpeptin-insensitive decrease in FRET. The solid red arrow in (c) indicates the `major drop of FRET' associated with calpain activation. (e) Onset times of DCD and calpain activation as compared to the application of glutamate. Boxes connected with lines indicate individual neurons exhibiting both DCD and calpain activation. Triangles indicate neurons with DCD but no calpain activation. (f) Mean ± SE of temporal cross-correlalograms comparing changes in FRET ratio to Fura-6F ratio. Data indicate mean ± SE of the cross-correlation diagrams calculated for neurons showing calpain activation in the vehicle-treated condition (f, n=23), and for neurons exhibiting DCD in the calpeptin-treated condition (g, n=49). Red arrows correspond to arrows in (c-d). Data were pooled from experiments using 5 different cell culture batches.

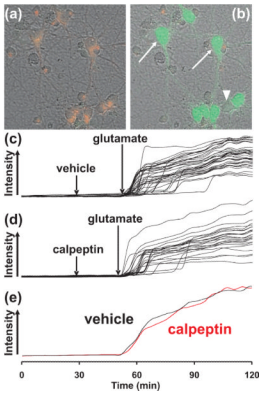

Fig 2. The effect of calpeptin on DCD in neurons imaged with Fluo-4FF

Neurons loaded with the membrane potential sensitive dye $TMRM^+$ (red) and the calcium indicator Fluo-4FF (green) are depicted before (a) and 16 minutes after (b) treatment with 100 μM glutamate. Arrows identify examples of cells with intense Fluo-4FF fluorescence that underwent calcium deregulation while the arrowhead denotes a cell that did not yet exhibit DCD although it depolarized in response to glutamate. In (c-d), Fluo-4FF responses in individual cells from representative fields of neurons are plotted over time in the absence (c) and presence (d) of 10 μM calpeptin. (e) shows the average $[Ca^{2+}]_c$ response from each field of cells.

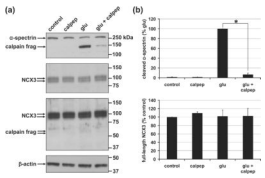

Fig. 3. Calpain-dependent, calpeptin-sensitive processing of α-spectrin but not NCX3

(a) Representative immunoblots depict levels of α-spectrin (first panel) and NCX3 (second and third panels) in whole cell lysates. The third panel is a longer exposure of the second panel. The 150 and 145 kilodalton (kDa) calpain cleavage products of α-spectrin are identified while breakdown products of NCX3 relative to full-length NCX3 could barely be detected even when films were overexposed (third panel). An immunoblot for β-actin (fourth panel) served as a loading control. (b) Densitometric quantification of the results represented in (a) following normalization to β-actin (mean ± SE, n=3). The asterisk indicates a significant effect of calpeptin + glutamate relative to glutamate alone ($p<0.05$).

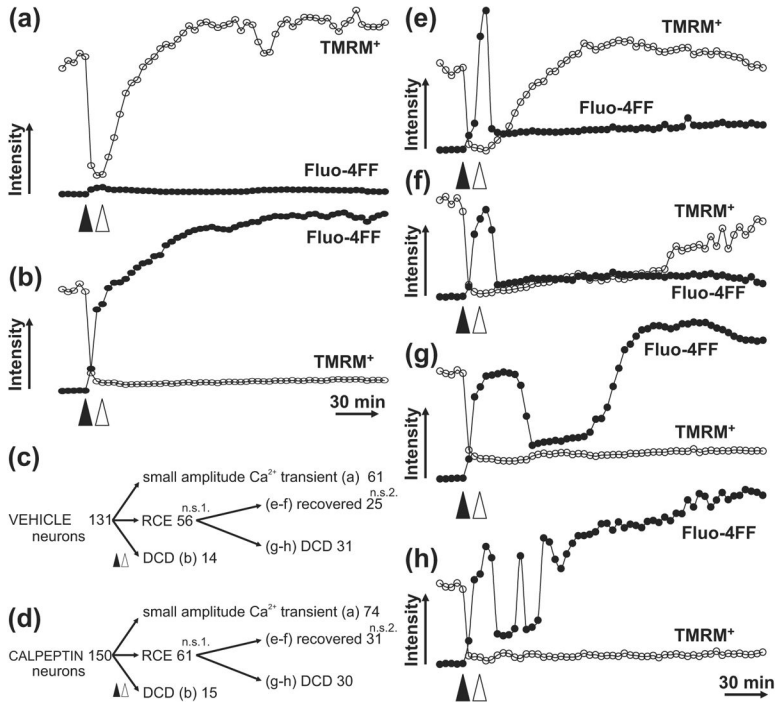

Fig. 4. Reversible calcium elevation (RCE) induced by transient glutamate exposure occurs with variable recovery

$TMRM^+$ (-o-) and Fluo-4FF (-•-) responses are depicted in representative cells undergoing $[Ca^{2+}]_c$ changes from 4 independent experiments. Glutamate (100 μM) was added at the solid arrowheads and glutamate receptor activation was terminated by the addition of MK801 (10 μM) and NBQX (10 μM) after 12 min (open arrowheads). A typical neuron exhibiting a small calcium transient without RCE or DCD is depicted in (a), irreversible DCD is shown in (b), and (e-h) depict cells with RCE. The cells in (e) and (f) recover $TMRM^+$ with fast or slow kinetics, respectively, without subsequent DCD. The cells in (g) and (h) undergo DCD without $TMRM^+$ recovery after single (g) or multiple (h) RCE events. The diagrams in (c) and (d) visualize the total number neurons in each category for vehicle (c) and calpeptin (d; 10 μM) treated cultures. Data were pooled from 4 independent experiments; n.s., not significant with Fisher's exact test comparing vehicle and calpeptin treatments and the number of neurons exhibiting RCE (1) or complete recovery (2).

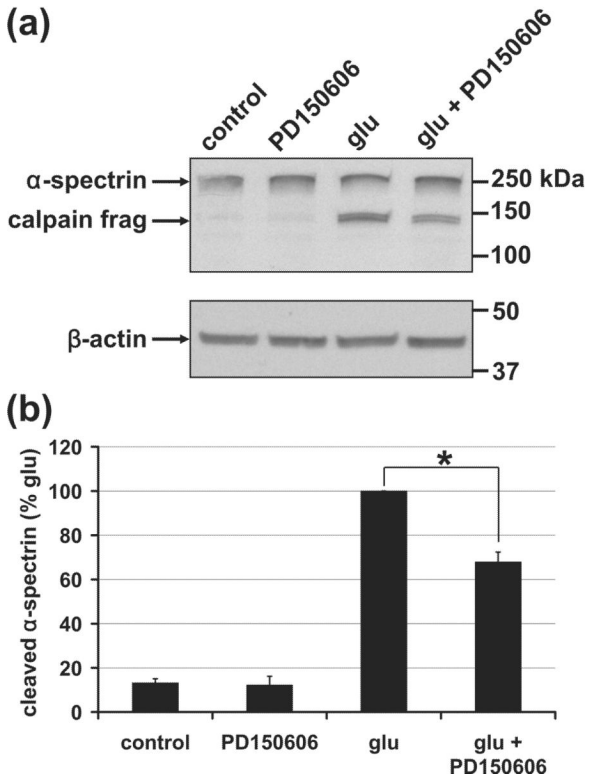

Fig. 5. Inhibition of> α-spectrin proteolysis by PD150606

(a) Representative immunoblot depicting full-length and calpain cleaved α-spectrin in whole cell lysate (upper panel), with β-actin as a loading control (lower panel). (b) Densiometric quantification of the results represented in (a) following normalization to β-actin (mean ± SE, n=3). The asterisk indicates a significant effect of 50 μM PD150606 + glutamate relative to glutamate alone ($p<0.05$).

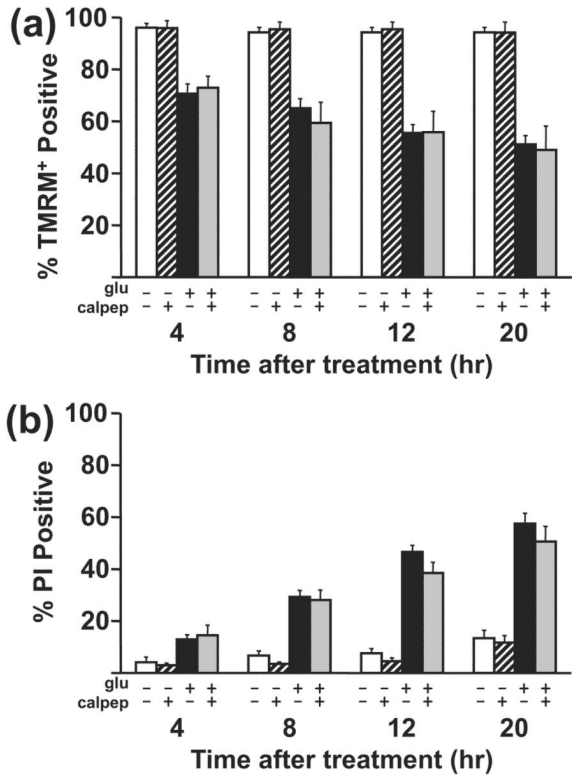

Fig. 6. Effect of calpeptin on cell death following a 30 min glutamate challenge

Cortical neurons received a 30 min 100 μM glutamate or mock challenge with or without a 30 min calpeptin pre-treatment (white bars, control, hatched bars, calpeptin, black bars, glutamate, gray bars, glutamate + calpeptin). The glutamate challenge was ended by the addition of 10 μM MK801 + 10 μM NBQX. Cell viability and death over time were monitored by $TMRM^+$ and propidium iodide fluorescence, respectively, and quantified at 4, 8, 12, and 20 hrs after the end of the glutamate challenge. For $TMRM^+$ data, mean ± SE is from n=4 wells for control ± calpeptin and from n=6 wells for glutamate ± calpeptin, both from 4 independent cultures. For PI data, mean ± SE is from n=10 wells for control ± calpeptin and from n=12 wells for glutamate ± calpeptin, both from 7 independent cultures. Glutamate and calpeptin were present throughout.

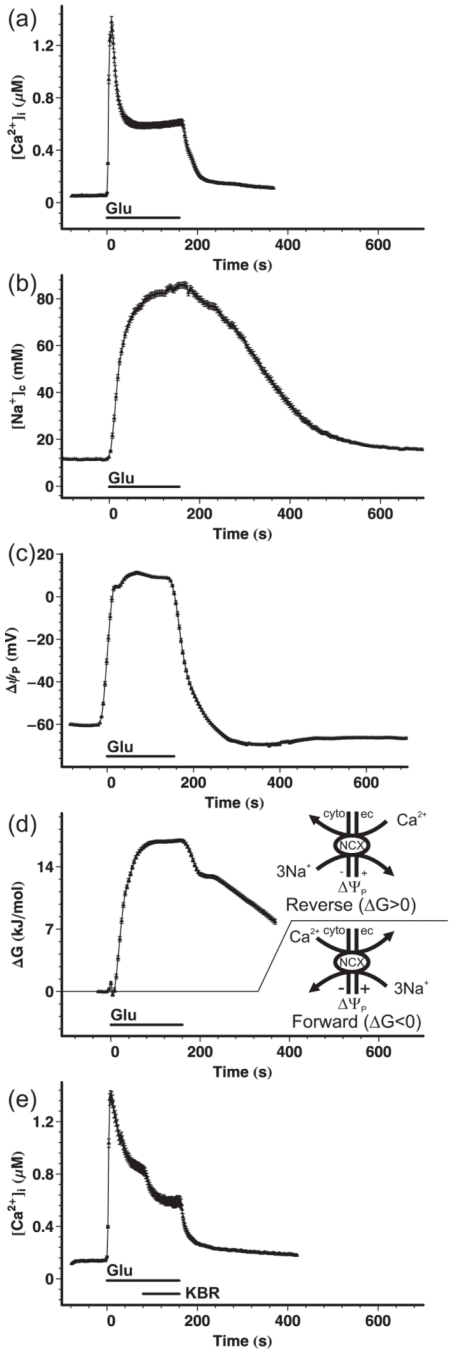

Fig. 7. Reversal of the NCX during glutamate treatment of cortical neurons

(a-c) Cortical neurons were wide-field fluorescence imaged to quantify the glutamate-triggered rise of $[Ca^{2+}]_c$ with Fura-4F (a) and in separate experiments the rise of $[Na^+]_c$ (b) and the depolarization of the $\Delta\Psi_P$ (c), using SBFI and PMPI, respectively. Glutamate (100 μM) plus glycine (10 μM) were applied in the absence of Mg^{2+} with a perfusion system (Glu), and then were washed out with Mg^{2+}-containing (1 mM) experimental medium. (d) The thermodynamic driving force of the NCX was calculated from the data shown in (a-c). The $[Ca^{2+}]_e$ and $[Na^+]_e$ were 1.3 mM and 136 mM respectively. A negative ΔG was defined as the forward mode of exchange; i.e. pumping Ca^{2+} out from the cell, while positive ΔG indicates reversal of the NCX. (e) Effect of the reverse-mode NCX inhibitor KB-R7943

(KBR; 10 μM) on the glutamate-triggered $[Ca^{2+}]_c$ plateau. Drug application was performed with a perfusion system with nifedipine (1 μM) continuously present in all perfusion lines. Data are mean ± SE of neurons pooled from 6 experiments per condition performed in 3 cell culture preparations (n=385, 202, 202, and 169 for (a), (b), (c), and (d), respectively). The SE in (d) was propagated from (a-c).

Table 1

Incidence of glutamate-induced DCD in the presence of calpain or NCX inhibitors relative to same-day controls

Treatment	% O_2 of culture	% DCD at 20 min	% DCD at 60 min	# of cells	# of view fields
calpeptin (10 μM)	3	109.9 ± 6.7*	115 ± 6.4*	705	27
PD150606 (10 μM)	3	68.2 ± 14.0	83.1 ± 8.4	384	6
PD150606 (50 μM)	3	11.8 ± 4.8*	44.7 ± 11.8*	300	6
KB-R7943 (10 μM)	3	31.4 ± 10.7*	57.6 ± 11.7*	348	6
calpeptin (10 μM)	20	125.7 ± 10.6*	112.2 ± 4.3*	590	18
PD150606 (10 μM)	20	71.8 ± 7.1*	92.0 ± 6.2	303	6
PD150606 (50 μM)	20	17.0 ± 3.4*	41.0 ± 6.1*	302	5
KB-R7943 (10 μM)	20	56.1 ± 9.4*	77.8 ± 10.9	312	6

Nifedipine (1 μM) was present in experiments with KB-R7943 to exclude the possibility that action was due to effects on voltage-dependent Ca^{2+} channels. Significance was determined by comparing the relative incidence of DCD in n view fields to 100% using a two-tailed Student's t-test.

*$p<0.05$